Sequential Spin Polarization of the Fermi Surface Pockets in URu_{2}Si_{2} and Its Implications for the Hidden Order

M. M. Altarawneh, N. Harrison, S. E. Sebastian, L. Balicas, P. H. Tobash, J. D. Thompson, F. Ronning, and E. D. Bauer

Phys. Rev. Lett. **106**, 146403 — Published 7 April 2011

DOI: 10.1103/PhysRevLett.106.146403

Sequential spin polarization of the Fermi surface pockets in URu_2Si_2 and its implications for the hidden order

M. M. Altarawneh[1], N. Harrison[1], S. E. Sebastian[2], L. Balicas[3],
P. H. Tobash[1], J. D. Thompson[1], F. Ronning[1] and E. D. Bauer[1]
[1]*Los Alamos National Laboratory, MS E536, Los Alamos, New Mexico 87545*
[2]*Cavendish Laboratory, Cambridge University, JJ Thomson Avenue, Cambridge CB3 OHE, U.K*
[3]*National High Magnetic Field Laboratory, East Paul Dirac Drive, Tallahassee, Florida 32310*

Using Shubnikov-de Haas oscillations measured in URu_2Si_2 over a broad range in magnetic field 11 - 45 T, we find a cascade of field-induced Fermi surface changes within the hidden order phase I and further signatures of oscillations within field-induced phases III and V [previously discovered by Kim *et al.*; Phys. Rev. Lett. **91**, 256401 (2003)]. A comparison of kinetic and Zeeman energies indicates a pocket-by-pocket polarization of the Fermi surface leading up to the destruction of hidden order phase I at ≈ 35 T. The anisotropy of the Zeeman energy driving the transitions in URu_2Si_2 points to an itinerant hidden order parameter involving quasiparticles whose spin degrees of freedom depart significantly from those of free electrons.

The interplay between a lattice of local magnetic moments and a sea of itinerant carriers has been shown to give rise to complex phase diagrams and the possibility of unusual states of matter not realized in simple metals [1–3]. URu_2Si_2 has come to epitomize the richness of the physics that can result in strongly correlated materials [4], displaying multiple phase transitions as a function of temperature, pressure and magnetic field [5, 6]. One particularly odd aspect of URu_2Si_2 is that it undergoes a robust thermodynamic phase transition into an ordered phase below $T_o \approx 17.5$ K [7] that lacks a microscopic description despite numerous attempts at its characterization [8–14]. It has become to be known as the 'hidden order' (HO) phase following the postulated existence of similarly elusive hidden orders in the cuprates [15].

While some aspects of the ordering in URu_2Si_2 can be understood from the perspective of local moments decoupled from the conduction sea [9, 16, 17], others – such as the quasiparticles having effective masses many times heavier than free electrons – indicates $5f$-electron participation in the Fermi surface [18, 19]. One possibility gaining momentum in recent years is that the small pockets result from Fermi surface reconstruction by a density-wave HO [8, 20, 21]. If true, one should expect such pockets to be particularly sensitive to the coupling of a magnetic field H to the quasiparticle spin [22]. Evidence for a field-induced Fermi surface change within the HO phase has been reported [23, 24]. Yet experiments to date have been performed over restricted intervals in H, leaving the driving mechanism unidentified.

In this paper, we report Shubnikov-de-Haas (SdH) oscillations in a high quality single crystalline sample measured over an broad range of field $11 \leq \mu H \leq 45$ T, enabling previous Fermi surface studies performed over different ranges in field to be reconciled. We identify a cascade of Fermi surface changes within the HO phase and signatures of continued oscillations within field-induced HO phases III and V. A comparison of the kinetic and Zeeman energies of the pockets suggests a sequential polarization of the Fermi surface, culminating in the destruction of the HO phase at ≈ 35 T. The implications for the HO parameter are discussed.

URu_2Si_2 is grown using the Czochralski technique, processed by electrorefinement and cut to yield a single crystal with a residual resistivity ratio of ≈ 400 between 2 and 298 K. The phase diagram is verified using contactless conductivity methods in pulsed magnetic fields [25] to match that of prior studies [5]. For dilution refrigerator magnetotransport measurements at the National High Magnetic Field Laboratory (NHMFL), the sample is polished down to $3 \times 0.3 \times 0.1$ mm^3 (the latter dimension referring to the c-axis).

Figure 1 shows the magnetoresistance measured over a broad range in magnetic field at ≈ 60 mK. While its overall form closely resembles that of earlier studies [23, 24], the SdH oscillations found here are larger in amplitude, exhibiting several distinct changes in the waveform as a function of the applied magnetic field H. In phases III and V the oscillations are greatly suppressed in amplitude, while above ≈ 39 T they become unobservable owing to the ≈ 400-fold reduction in resistivity.

Changes in the waveform of the oscillations at ≈ 17, 24 and 29 T are reflected in their spectral content, provided by Fourier transforms in Fig. 2. Oscillations in the low field regime (I_A in Fig. 2**a**) correspond closely to those originally measured by Ohkuni *et al* [19], and more recently measured by Hassinger *et al.* [26], over a similar region in field, both with respect to the values of the quantum oscillation frequencies F and fitted quasiparticle effective masses m^* (shown in Fig. 2 insets and summarized in Table I). In region I_B, above a characteristic field of ≈ 17 T (at which the magnetoresistance deviates from quadratic behavior [24]), we find the frequencies to be shifted by a few tens of teslas – accounting for the differences in frequency observed between Shishido *et al.* [24] and Ohkuni *et al.*. More significant changes in

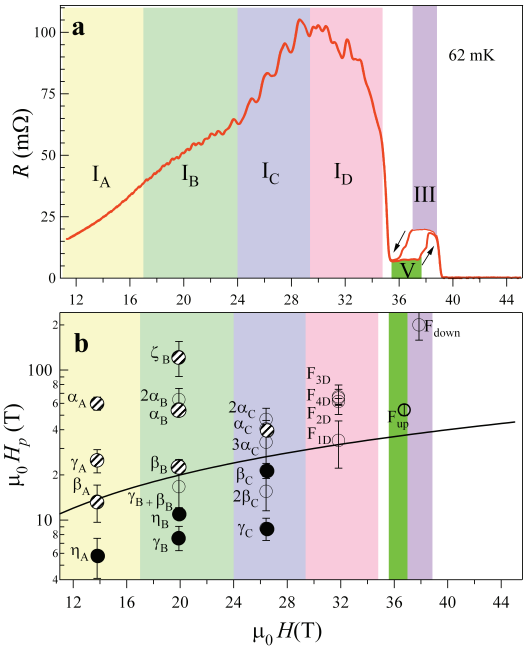

FIG. 1: **a**, Magnetoresistance of URu_2Si_2 on the rising and falling magnetic field (indicated by arrows) showing HO phases I, III and V in which SdH oscillations are seen. 4 regions (I_A, I_B, I_C and I_D) are identified within phase I, each revealing different SdH frequencies (see Fig. 2). **b**, A comparison of the field H_p defined in Eqn. (1) at which each pocket is expected to become spin-polarized (using the local value of F and m^*) with $1/\overline{(1/H)}$ in each region. Polarized pockets (filled symbols) fall well below the solid line. Unpolarized pockets (striped symbols) lie on or above the line. Open symbols refer to harmonics, combination frequencies or frequencies observed at $\mu_0 H > 29.4$ T where the polarization state can no longer be reliably determined owing to the nonlinear magnetization [27]. Note that the inverse field interval in region I_C is too short to resolve η.

F are then observed above ≈ 24 T (at which the slope of the magnetoresistance increases [24]) within the region denoted I_C, thus accounting for the different frequencies reported by Jo *et al.* [23]. Finally, the oscillations take on a chaotic appearance beyond ≈ 29 T in region I_D where the magnetoresistance is negative. Our ability to resolve separate frequencies in I_D is limited by the range in $1/H$ – hence the different labels.

	I_A	I_B	I_C	I_D
α, F_{2D}	1050 (14)	1000 (14)	890 (17)	1200 (15)
β, F_{1D}	450 (25)	490 (17)	560 (20)	510 (10)
γ	220 (7)	250 (25)	230 (20)	-
η	90 (13)	120 (8)	-	-
ζ	-	1510 (10)	-	-

TABLE I: Summarized values of F for each region within HO phase I from Fig. 2, with m^* shown in parenthesis.

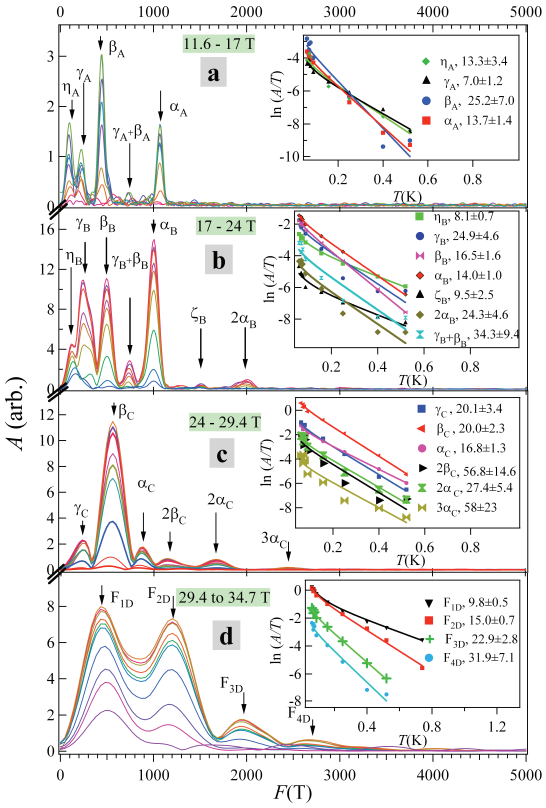

FIG. 2: **a** - **d**, Fourier transforms (using a Hanning window) in each HO phase I regime identified in Fig. 1**a**. The frequencies in regions I_A and I_B are labeled according to Ohkuni *et al.* [19] and Hassinger *et al.* [26], while ζ is newly identified. Insets show estimates of m^* for the various orbits and combination frequencies obtained by fitting to $A = A_0 X/\sinh X$ [32] where $X = 2\pi^2 m^* k_B T/\hbar e B$. Harmonics and combination frequencies are inferred from the values of F and m^*.

A clue as to the origin of the changes in F is provided by the heavy masses of the quasiparticles compared to the small sizes of the pockets. In the case of the η orbit observed in region I_A, for example, F and m^* imply a band filling of $\varepsilon_\eta = \hbar e F/m^* \approx 0.8$ meV (assuming a parabolic band) that is significantly lower than the Zeeman energy scale $h = \frac{1}{2} g \mu_B \mu_0 H \approx 1.3$ meV (for $g \approx 2$) at the lowest applied field of ≈ 11 T. Spin polarization of the smallest pocket η in weak magnetic fields is therefore implied (see schematic in Fig. 3).

For an effective g-factor g^* specific to URu_2Si_2, we turn to the angle-dependent de Haas-van Alphen measurements of Ohkuni *et al.* [19] and their subsequent analysis in Ref. [33]. While the determination of the effective g-factor in f-electron materials is often made complicated by the spin-dependence of m^* and scattering rate [34–36], URu_2Si_2 proves to be a simple exception – 16 spin zeroes are observed in the amplitude on rotating the field from the c-axis by an angle θ [19], enabling the θ-dependence of g^* to be mapped to unprecedented detail [32]. Each

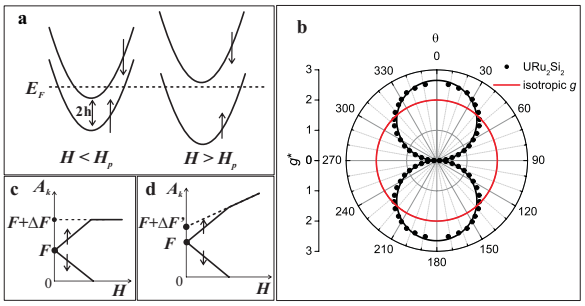

FIG. 3: **a**, Schematic showing band polarization caused by Zeeman splitting, resulting in the depopulation of the minority spin component above $H_{\rm p}$ defined in Eqn (1). **b**, Polar plot of the measured θ-dependent effective g-factor in URu_2Si_2 [19, 33] (black symbols) together with a fit to $g^* = g_z \cos\theta$ (black line), where $g_z = 2.6$ (assuming $\frac{1}{2}$ pseudospins), and its comparison with an isotropic $g = 2$ (red line). **c**, Schematic of the field-dependent cross-sectional areas of the up and down-spin components for a single pocket, together with the 'back projected' quantum oscillation frequency before F and after $F + \Delta F$ polarization. **d**, The same schematic in which the frequency shift $\Delta F'$ is reduced by additional pockets acting as a charge reservoir.

spin zero (l) corresponds to an odd integer value $(2l+1)$ of the product $m^*g^*/m_{\rm e}$ (where $m_{\rm e}$ is the free electron mass) at which the two spin contributions destructively interfere. On plotting the θ-dependence of g^* obtained after dividing this product by the measured θ-dependent m^* [19], g^* can be seen to be extremely anisotropic compared to that $g \approx 2$ of free electrons. Such anisotropy implies that the spin quantum numbers of the local $5f^2$ moments in URu_2Si_2 are incorporated into the Fermi surface by their hybridization with the conduction sea [33]. While $g^* \approx 0$ when H lies in the planes, reflecting the vanishing Pauli susceptibility at that orientation, it rises to a large value $g^* \approx 2.6$ when H is aligned along the c-axis (as in the current experiment) causing spin polarization to become a significant factor. In Fig. 1**b** we use $g^* \approx 2.6$ to estimate the field

$$\mu_0 H_{\rm p} = \frac{2Fm_{\rm e}}{m^*g^*} \qquad (1)$$

at which each pocket is expected to become spin polarized. On comparing $H_{\rm p}$ with the average inverse applied magnetic field $1/\overline{(1/H)}$ within each region, the frequency shifts taking place on entering regions I_B and I_C can be seen to be associated with the consecutive polarization of pockets γ and β (with η already being polarized for $\mu_0 H \ll 11$ T). The observed spin zeroes in URu_2Si_2 [19] reinforce the validity of Eqn (1), implying linear Zeeman splitting and spin-independent masses.

To understand how polarization affects the observed frequencies, we turn to the schematic in Fig. 3**c**. When $H < H_{\rm p}$, the linearly Zeeman split pocket areas yield a constant 'back projected' frequency $F = -H^2(\frac{\hbar}{2\pi e})\frac{\partial}{\partial H}(\frac{A_k}{H}) = (\frac{\hbar}{2\pi e})A_0$ [35], where A_0 is the area at $H = 0$ [28]. Once $H > H_{\rm p}$, however, the areas no longer change with H (for a single isolated pocket), giving rise to a back projected frequency $F + \Delta F \approx \sqrt[3]{4}F$ for the majority spin component shifted from its original value. Here, we assume ellipsoidal pockets whose k-space volumes for a single spin are double those for two spins.

Polarization causes the chemical potential μ to vary linearly with field above $H_{\rm p}$. If there are additional pockets present, as in URu_2Si_2, then their combined density-of-states $\sum_i \gamma_i$ (where $\gamma_i \propto n\sqrt{F}m^*$ [26] is the contribution from individual pockets $i = \alpha$, β, γ, η and ζ) acts as a charge reservoir causing carriers to flow between pockets, weakening the field-dependence of μ. The reservoir affects the F shifts in two ways. First, the weakened change in slope of A_k versus H at $H_{\rm p}$ (see Fig. 3**d**) reduces the shift of the pocket being polarized to $\Delta F' \sim \Delta F \times (\frac{\gamma_i}{\sum_i \gamma_i})$. Second, the remaining field-dependence of μ causes *all* pockets to experience a change in the slope of A_k versus H, causing *all* frequencies to shift at $H_{\rm p}$ – the sign of the shift being opposite for opposing carrier types (with the shifts accumulating as each pocket becomes polarized). The shift of α and β in opposite directions is explained by their respective association with electron and hole pockets [12, 26, 31]. On assuming all pockets to occur once in the Brillouin zone such that $n = 1$, with the exception of β for which $n = 4$ [12, 26], we obtain $\Delta F' \sim 20$ T and 150 T for the polarization of γ and β respectively. We can now understand why the second frequency shift (between I_B and I_C) involving the β pocket polarization is larger than the first (between I_A and I_B) in Fig. 2– the β pocket represents a significantly greater fraction of the total density-of-states.

The non-linear magnetic susceptibility [27, 29] and accumulating frequency shifts likely reduce the accuracy of Eqn (1) in the limit $\mu_0 H \to 35$ T. On the other hand, the irregular appearance of the SdH waveform, the downward trend in $H_{\rm p}$ versus H (see Fig. 1**b**) and the significant changes in the Hall effect [30] suggest that α becomes polarized in region I_D. It is therefore likely that the polarization of the majority of the Fermi surface precedes the destruction of the HO phase I at ≈ 35 T [29]. Finally, in Fig. 4 we turn to the oscillations in phases V and III for which hysteresis (see Fig. 1**a**) [5] causes the field interval within each phase to become dependent on the field sweep direction. The spacing in $1/H$ between consecutive oscillations corresponds to dominant frequencies of ~ 2 kT and ~ 3 kT in phases V and III respectively, suggestive of a significant changes in Fermi surface topology accompanying each metamagnetic transition [5, 27]. Lifshitz-Kosevich behavior of the oscillations is evidenced by their temperature dependences (see Fig. 4).

In summary, we observe field-induced SdH frequency changes occurring at several different fields ($\approx$ 17, 24 and 29 T) within the HO phase and find these to be consistent with a sequential spin polarization of the small

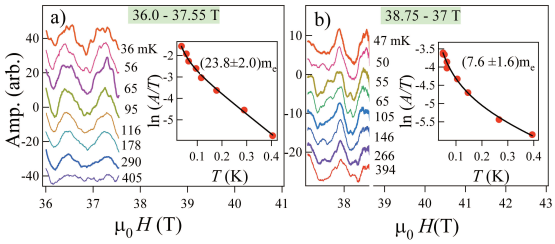

FIG. 4: **a** and **b**, Oscillations in phases V and III, respectively, at different temperatures as indicated (listed in order). The insets show fits to estimate m^*, with the amplitude at each temperature determined by Fourier analysis.

Fermi surface pockets in URu_2Si_2. Spin polarization of the Fermi surface therefore appears to be the primary factor responsible for the destruction of HO phase I at $\approx$ 35 T. More abrupt Fermi surface changes occur on entering thermodynamically distinct phases III and V, previously identified by Kim *et al.* [5].

The highly anisotropic effective g-factor of the quasiparticles driving the transition(s) points to a HO parameter that is itinerant in nature, involving $5f$-electron spin degrees of freedom that are fully integrated into the Fermi surface. The latter has important implications for the HO, given the direct correlation between the degrees of freedom of the itinerant quasiparticles and the degrees of freedom subject to ordering within a density-wave picture. The possibility of a density-wave order parameter involving unconventional spin or multipolar degrees of freedom [16] is suggested by the close similarity of the anisotropic effective quasiparticle g-factor to that expected for local non-Kramers Γ_5 doublets [17].

MMA and NH acknowledge the provision of the U.S. Department of Energy (DOE), Office of Basic Energy Sciences (BES) funding for the "Science of 100 Tesla." MMA further acknowledges a Seaborg fellowship. LB is supported by DOE-BES through award DE-SC0002613. Work by PHT, FR, JDT, and EDB is supported by the US DOE, Office of BES, MSE Division and by the LANL LDRD program. Experiments were performed at the NHMFL, which is supported by the US DOE, the National Science Foundation and the State of Florida.

[1] F. Levy *et al.* Science **309**, 1343 (2005).
[2] T. Park *et al.* Nature **440**, 65 (2006).
[3] M. Kenzelmann *et al.* Science **321** 1652 (2008).
[4] R. J. Hemley, G. W. Crabtree, M. V. Buchanan, Physics Today **62**, 32 (2009).
[5] K.-H. Kim *et al.* Phys. Rev. Lett. **91**, 256401 (2003); *ibid.* 206402 (2004).
[6] H. Amitsuka *et al.* J. Magn. Magn. Mater. **310**, 214 (2007).
[7] T. T. M. Palstra *et al.* Phys. Rev. Lett. **55**, 2727 (1985).
[8] P. Chandra *et al.* Nature **417**, 831 (2002).
[9] A. Kiss, P. Fazekas, Phys. Rev. B **71**, 054415 (2005).
[10] C. M. Varma, L. J. Zhu, Phys. Rev. Lett. **96**, 036405 (2006).
[11] J. Quintanilla, A. J. Schofield, Phys. Rev. B **74**, 115126 (2006).
[12] S. Elgazzar *et al.*, Nat. Mater. **8**, 337 (2009).
[13] K. Haule, G. Kotliar, Nat. Phys. **5**, 796 (2009).
[14] A. R. Schmidt *et al.* Nature **465**, 570 (2010).
[15] S. Chakravarty, R. B. Laughlin, C. Nayak, Phys. Rev. B **63**, 094593 (2001).
[16] H. Harima, K. Miyake, J. Flouquet, J. Phys. Soc. Japan **79**, 033705 (201).
[17] F. J. Ohkawa, H. Shimizu, J. Phys.-Cond. Matt. **46**, L519 (1999).
[18] C. Bergemann *et al.*, Physica B **230**, 348 (1997).
[19] H. Ohkuni *et al.* Phil. Mag. B **79**, 1045 (1999).
[20] P. A. Sharma *et al.* Phys. Rev. Lett. **97**, 156401 (2006).
[21] C. R. Wiebe *et al.* Nat. Phys. **3**, 96 (2007).
[22] A. Lebed, Ed. *The physics of organic superconductors and conductors* (Springer-Verlag, 2008).
[23] Y. J. Jo *et al.* Phys. Rev. Lett. **98**, 166404 (2007).
[24] H. Shishido *et al.* Phys. Rev. Lett. **102**, 156403 (2009).
[25] M. M. Alarawneh, C. H. Mielke, J. S. Brooks, Rev. Sci. Instr. **80**, 066104 (2009).
[26] E. Hassinger *et al.* Phys. Rev. Lett. **105**, 216409 (2010).
[27] N. Harrison, M. Jaime, J. A. Mydosh, Phys. Rev. Lett. **90**, 096402 (2003).
[28] The linear slopes of A_k versus H cause only a relative shift in phase between spin-up and -down quantum oscillations, resulting in the standard spin damping factor $R_s = \cos(\frac{\pi m^* g^*}{2m_e})$ [32].
[29] Consistent with polarization, the magnetization exhibits negative curvature at low fields, plus additional structure between $\approx$ 20 and 35 T. Once $\mu_0 H \rightarrow$ 35 T, the magnetization becomes dominated by an increase in the susceptibility approaching the hidden order phase I boundary.
[30] Y. S. Oh *et al.*, Phys. Rev. Lett. **98**, 016401 (2007).
[31] Hassinger *et al.* [26] have recently shown that the antiferromagnetic and HO Fermi surfaces are the same, suggesting that they share the same point group symmetry.
[32] D. Shoenberg, *Magnetic oscillations in metals* (Cambridge University Press, Cambridge 1984).
[33] A. V. Silhanek *et al.* Physics B **378**, 373 (2006).
[34] M. Endo *et al.* Phys. Rev. Lett. **93**, 247003 (2004).
[35] S. R. Julian, P. A. A. Teunissen, S. A. Wiegers, Phys. Rev. B **46**, 9821 (1992).
[36] A. A. Teklu *et al.* Phys. Rev. B **62**, 12881 (2000).